

Chapter 2

Visualizing the Bacterial Cell Surface: An Overview

Harald Engelhardt

Abstract

The ultrastructure of bacteria is only accessible by electron microscopy. Our insights into the architecture of cells and cellular compartments such as the envelope and appendages is thus dependent on the progress of preparative and imaging techniques in electron microscopy. Here, I give a short overview of the development and characteristics of methods applied for imaging (components of) the bacterial surface and refer to key investigations and exemplary results. In the beginning of electron microscopy, fixation of biological material and staining for contrast enhancement were the standard techniques. The results from freeze-etching, metal shadowing and from ultrathin-sections of plastic-embedded material shaped our view of the cellular organization of bacteria. The introduction of cryo-preparations, keeping samples in their natural environment, and three-dimensional (3D) electron microscopy of isolated protein complexes and intact cells opened the door to a new dimension and has provided insight into the native structure of macromolecules and the in situ organization of cells at molecular resolution. Cryo-electron microscopy of single particles, together with other methods of structure determination, and cellular cryo-electron tomography will provide us with a quasi-atomic model of the bacterial cell surface in the years to come.

Key words: Correlative microscopy, Cryo-electron microscopy, Cryo-electron tomography, Cryo-sectioning, Electron microscopy, Focused ion beam micromachining (FIB), Freeze-etching, Metal shadowing, Negative staining, Single particles, Template matching

1. From Staining to Visualization

Bacteria came into virtual existence in 1683 when Antoni van Leeuwenhoek detected *viva animalcula* in dental plaques by means of his self-made microscopes (1). Since then, microbiology has been intertwined with microscopy; and even in recent years, achievements of modern fluorescence microscopy and cryo-electron tomography founded a new (or revived an atrophied) discipline in microbiology, namely microbial cell biology. Investigations of the cellular organization and its compartments with new microscopies also shed light on the architecture of the microbial cell surface,

and of the bacterial cell envelope in particular, that is still being explored. 130 years ago and almost exactly 200 years after the initial observation of bacteria, Robert Koch developed a staining method to visualize and differentiate the causing agent of tuberculosis. Paul Ehrlich who improved the method shortly after interpreted the acid-resistant staining behavior as a specific property of the cell envelope (2) and thus realized that bacteria may have different cell wall compositions. The staining introduced by Hans Christian Gram in 1884 (3) had even more impact. It distinguished between two larger groups of microorganisms and was not only taken as indicative for the cell wall permeability (4) and thickness (5, 6) a number of decades later, but also for the apparent cell wall architecture of *gram-positive* (thick peptidoglycan, no outer membrane) and *gram-negative* bacteria (thin peptidoglycan, outer membrane in addition). However, cell envelopes turned out to be more diverse and the behavior of Gram staining often led to misinterpretations of the cell wall composition. The extreme chemical variability of the cell surface (mainly of lipopolysaccharides and flagellar antigens) became apparent by serological typing of *Salmonella* strains introduced in 1926 (7) and its systematic documentation based on the Kauffmann–White scheme (8), which meanwhile lists more than 2,500 entries (9). Staining and labeling methods for light microscopy have been and still are of diagnostic value but they could hardly reveal structural details of the bacterial cell surface because of the limited resolution power of light optical instruments.

The situation changed with the invention of transmission electron microscopy (EM) in 1932 (10), the first electron microscopical images of bacteria encouraging further studies (11, 12), and the development of appropriate preparation and imaging techniques (still in progress) that provided structural insights and prompted the research on microbial cell envelopes. Early investigations still employed staining methods known from cytology of eukaryotes (13). The era of fruitful investigations began in the early 1950s (14, 15), flourished in the 1960s and later when ultrathin sectioning had become a common method, and lasts until today, now profiting from cryo-electron microscopy of vitrified and unstained biological material in a close-to-native state. Any progress in the visualization of cell envelopes, their internal structure, and of its appendages preceded technical and preparative innovations. Major developments of EM after its invention (three-dimensional (3D) EM, cryo-electron tomography [CET]) occurred in about 30-years steps, as well as methods for specimen preparation (ultrathin sectioning, cryo-sectioning, cryo-focused-ion-beam micromachining [cryo-FIB]). Other significant improvements for imaging biological material, i.e., contrast and resolution enhancements (heavy metal shadowing, negative staining, EM of unstained material, zero-loss energy filtering, imaging correction by phase-plates) showed a periodicity of about 15 years, so that we observe a minor

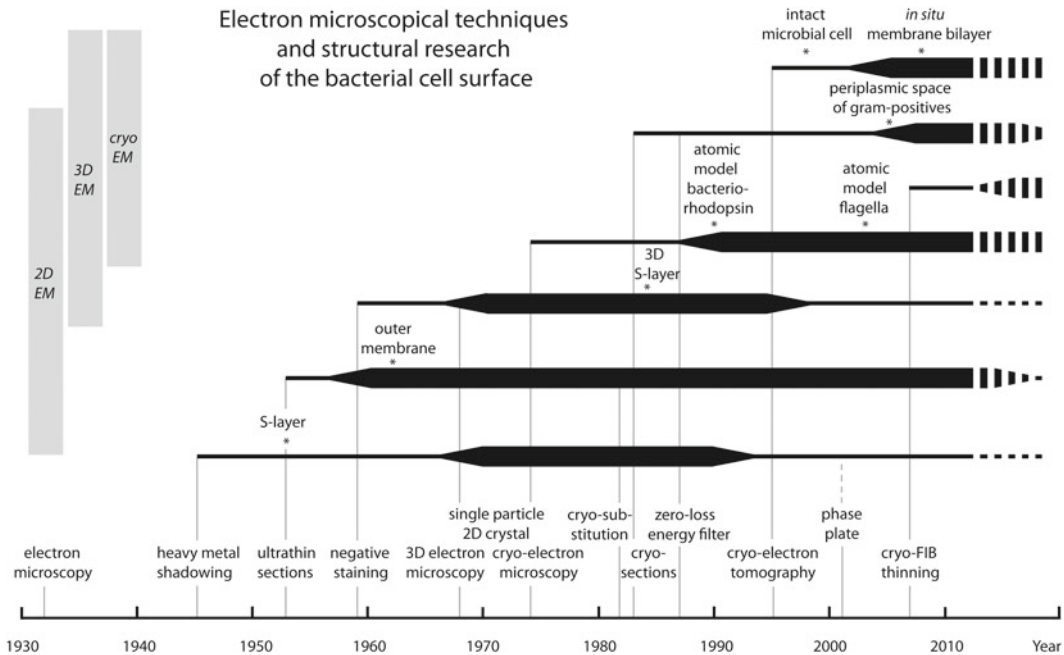


Fig. 1. Technical and preparative developments in transmission electron microscopy and their impact on structural research of microbial cell envelopes and their constituents. The *thickness* of time lines indicates the importance of methods. *Dashed lines* denote assessments for future applications. Some key discoveries in microbial surface structure research are indicated.

or major innovation step every 5–9 years that is of importance for structure research in (micro)biology (Fig. 1). The evolution of EM techniques was of course accompanied and partly driven by the immense progress of computational performance and efficient software solutions for image processing. The route led from chemically fixed, stained, and dehydrated specimens to native and vitrified preparations devoid of artificial modifications, from 2D projections to 3D reconstructions, and from low resolution images to quasi-atomic models for representative structures. Some important events of EM cell surface research are indicated in Fig. 1.

This chapter gives an overview of electron microscopical approaches, which have been of particular importance for structural research in microbiology, highlights its contributions to our understanding of the microbial cell surface, and outlines the perspectives for the near future.

2. Looking at Surfaces

2.1. Heavy-Metal Shadowing

Metal coating (“shadowing”) of isolated and dried cell envelopes was one of the first systematically applied contrasting methods (16, 17) when it had become clear that biological material

produced only low contrast in the EM. Metal shadowing led to the detection of regularly patterned cell wall layers (15, 18) in *Bacteria* and *Archaea* (as realized much later). The existence of these common surface layers (S-layers) was ignored in microbiology for a long time since neither *Escherichia coli* nor *Bacillus subtilis*, the bacterial model organisms, possess S-layers, and the classical ultra-thin sections often failed to display the complete profile of cell envelopes (see Subheading 3.1). Metal shadowing of S-layers became particularly attractive when the structural destabilization and heterogeneity of air-dried preparations was avoided by freeze-drying (19). The 2D crystalline assemblies, the use of metals with smaller grain size (e.g., tungsten–tantalum instead of platinum), the improved signal-to-noise ratio after image processing, and the recovery of the surface shape by relief reconstruction (20–22) stimulated a period of frequent studies (Figs. 1 and 2). The latter approach yielded reliable information on the surface structure of S-layers to about 2 nm resolution (23).

A technical variant, applying only low amounts of metal (gold, silver, platinum) that decorates preferred molecular sites but does not cover the whole surface, was used to identify and highlight periodic structures in freeze-dried or freeze-etched protein assemblies (24, 25). Metal shadowing and decoration of isolated material lost its appeal when 3D electron microscopy came into play (see Subheading 4). Today, contrasting by metal coating is used for some special applications only.

2.2. Freeze-Etching and Freeze-Fracturing

Cells, frozen as a whole, freed from ice by deep-etching (sublimation above -100°C), contrasted by metal coating, and finally prepared for EM by the replica technique (26–28), show their very surface. For a long time, this was the only method to look at cells from outside. Again, it was a useful approach for identifying and characterizing the outermost layer of bacterial cells. By this way the orientation of S-layers could be determined and comparisons with the isolated layer and its 3D reconstruction revealed conformational variations (upon isolation). Although informative, such comprehensive investigations remained scarce (Fig. 2, (29)).

Freeze-fracturing—where the frozen cells are broken prior to etching and metal coating—not only displayed cell surfaces but also part of the envelope profile. Since fracture faces propagate along surfaces and hydrophobic ones in particular, often the inner or outer leaflet of membranes was visible and thus indicative of lipid membranes (30).

2.3. Scanning Electron and Scanning Probe Microscopy

Imaging of surface structures from abiotic and biological material is an original domain of scanning electron microscopy (SEM). This approach usually also employs metal coating and is limited in lateral resolution for several reasons so that molecular details of cell surfaces can hardly be investigated (31). Therefore, SEM does

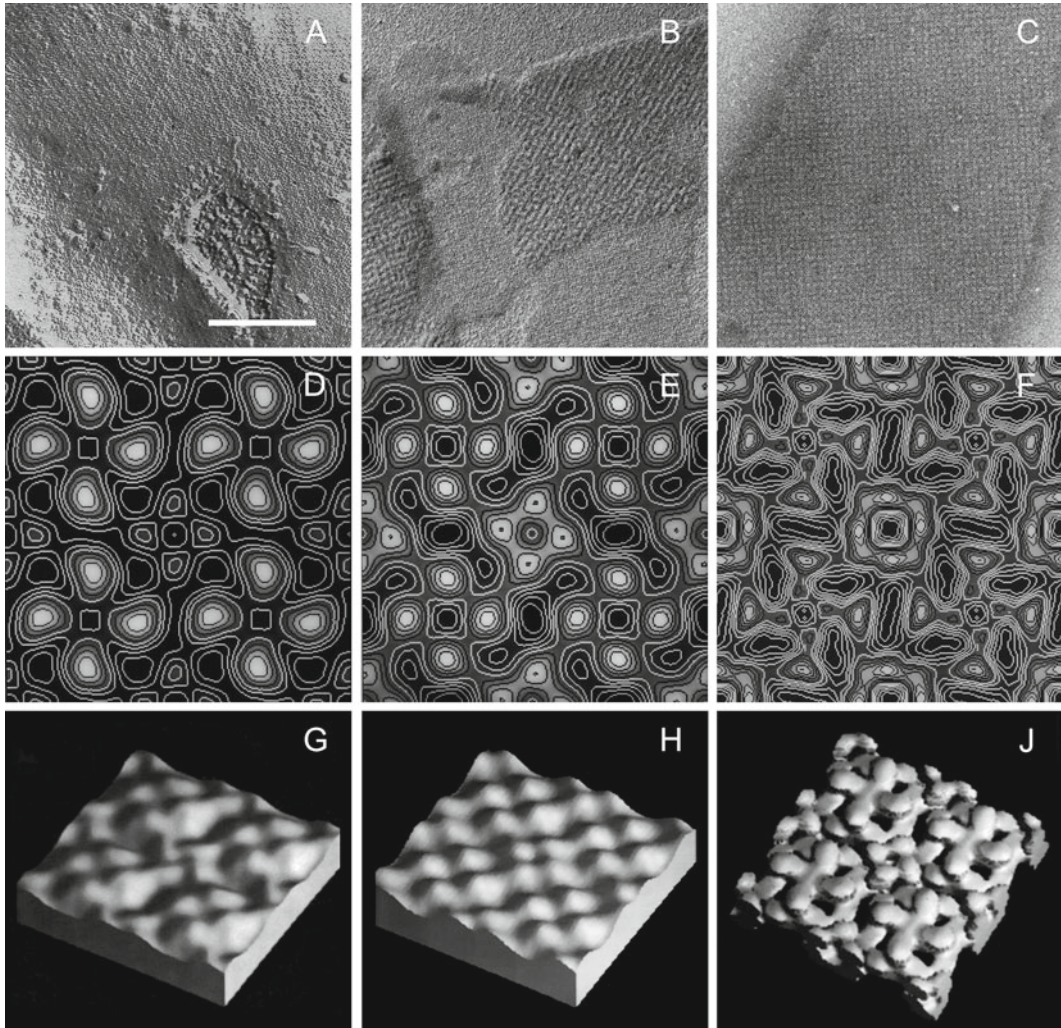


Fig. 2. Staining and reconstructions of the S-layer from *Sporosarcina ureae*. (a, d, g) Freeze-etched cell unidirectionally shadowed by tungsten-tantalum. (b, d, h) Isolated S-layer unidirectionally shadowed by tungsten-tantalum. (c, f, i) Isolated S-layer negatively stained with Na/K-phosphotungstate. (d, e) Surface relief reconstruction of the outer surface after averaging of unit cells; *contour lines* indicate identical levels of the relief height (*black* areas are valleys). The central tetragonal domain has a different height in the isolated S-layer and indicates a conformational change upon detachment from the cell wall. (f) Averaged S-layer lattice; *black* areas indicate stain-filled gaps, *bright* areas represent protein mass. (g, h) Models of reliefs from the outer surface. (i) Three-dimensional (3D) (isosurface) model of the S-layer based on tilt-series data. Scale bar indicates 200 nm (valid for a–c). The averages and models (d–i) show four unit cells each (lattice constant 12.9 nm).

not play a prominent role in studies of the bacterial surface although low-voltage SEM promises interesting applications in biology (32).

In the 1980s, a novel type of microscopy was invented and introduced a fascinating approach to gain topographical and spectroscopic information from surfaces, i.e., scanning probe microscopy (SPM) (33, 34). Atomic force microscopy (AFM) of fully hydrated and uncoated protein assemblies, once more of S-layers

(35, 36), and membranous samples containing densely packed protein complexes (2D crystalline porins (37)), yielded topographical images of high signal-to-noise ratio, so that single complexes could be inspected. AFM has an impressive z-resolution down to 1 Å and a subnanometer resolution in *x-y*-direction, depending on the tip geometry and the structure of the sample (38, 39). Functionalization of the tip and particular scanning modes allow for probing various molecular features such as polarity and charges (40), hydrophobicity, elasticity or roughness (41), and can be applied to probe molecular forces for binding and unfolding (42, 43). Investigations of the surface of intact cells are possible (44); but—according to a hidden law—the larger the object under the tip the weaker the resolution of details. The preferred domain of SPM for topographical investigations is flat specimens such as membranes and densely packed proteins with moderate corrugation that firmly adhere to the supporting substrate. Similar to other approaches probing *surface* characteristics, scanning microscopies are complementary to methods for *3D structure* analysis.

3. Profile of Cell Envelopes

3.1. Ultrathin Sectioning: Looking into Microbes

Intact bacteria, either directly dried or soaked with (heavy) metals were not suited for EM because of the extremely low or high contrast, preventing imaging of details (45). The solution to this problem was thin-sectioning, a technique that was already known from preparations of tissues. However, the sections had to be ultrathin (≤ 100 nm) and this required the development of new microtomes (14, 46, 47). In the 1960s and 1970s the common methods for fixation (glutaraldehyde), dehydration (water-ethanol exchange), staining (OsO_4 , $\text{Pb}(\text{OH})_2$, ruthenium red), embedding (epoxid resins), and polymerization (60°C) were established and represented the basis for most of the cytological investigations in the following two decades. In the early 1960s, the existence of an outer membrane became apparent (48–50) and the characteristic difference of the cell wall thickness of gram-positive and gram-negative bacteria was established. The development and peculiarity of the architectural layers cytoplasmic membrane, peptidoglycan, outer membrane, polysaccharide capsules (slime), and sometimes other (unidentified) components were investigated and shaped our view of the composition and variability of the bacterial cell envelope (31, 51). Interestingly, S-layers were only rarely detected or recognized in ultrathin sections (52). One of the reasons was that they usually did not show up very clearly—with some remarkable exceptions (53–55)—and another one that microbiologists were not prepared to *perceive* this structure (56). A systematic investigation of the staining behavior of ultrathin sections from *Deinococcus*

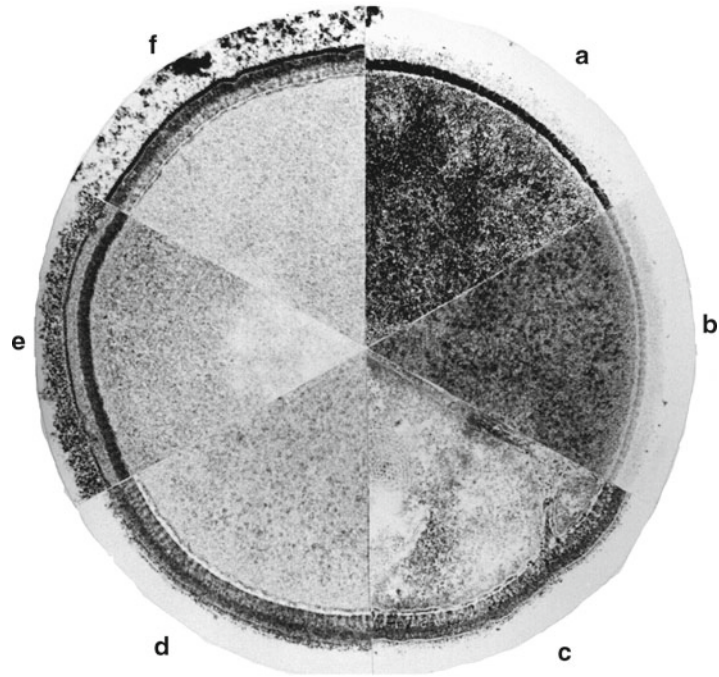


Fig. 3. Effect of different fixation and staining conditions for ultrathin sections of *Deinococcus radiodurans*. The cells were treated with (a) OsO_4 and PbO , (b) glutaraldehyde, OsO_4 , and Pb(OH)_2 , (c) tannin, OsO_4 , and Pb(OH)_2 , (d) tannin, glutaraldehyde, OsO_4 , and Pb(OH)_2 , (e) glutaraldehyde, OsO_4 , ruthenium red, and Pb(OH)_2 , (f) tannin, glutaraldehyde, OsO_4 , ruthenium red, and Pb(OH)_2 . All samples were embedded in epoxide resin and polymerized at 60°C . Most of the sections show the thick fenestrated peptidoglycan, but only the section in (d) indicates the existence of an outermost layer possessing a periodic structure (S-layer “HPI”) (Courtesy of W. Baumeister, Martinsried).

radiodurans—possessing a thick fenestrated peptidoglycan, an outer membrane, an S-layer, and a polysaccharide capsule (57)—illustrates the impact of preparation conditions for the visualization of cell envelope components and for the interpretation of the cellular architecture (Fig. 3).

Another problem was the harsh preparation conditions that were suspected to alter the appearance of morphological details and to denature protein complexes. The structural integrity of cells was improved by cryo-substitution and new embedding materials, polymerizing in the cold (58). Hence, proteins were conserved better and could be localized by immuno-EM easier than before (59). Today, this is the standard procedure for bacteria, ideally being combined with high-pressure freezing for improved structural preservation. However, substitution of cellular water and staining, even in the cold, could still not be expected to keep the organization of macromolecules untouched. If a near-to-life situation has to be guaranteed there is no way other than freezing the samples and keeping them frozen in the microscope without any chemical treatment.

3.2. Cryo-Sectioning: Pure Nature

As early as 1960, Humberto Fernández-Morán explored methods for cryo-electron microscopy (60). Yet, it took another two decades until basic experiments encouraged the development of cryo-sectioning to a reproducible and reliable technique (61–63). As an important prerequisite, Jaques Dubochet demonstrated that quick freezing prevents water from forming ice crystals that would destroy the (molecular structure of) biological samples otherwise; water could be *vitrified* (64). Vitrification is possible by plunge-freezing (fast injection of samples into a cryogen such as ethane at $\approx -180^\circ\text{C}$ (65)) if the specimen thickness does not exceed $\approx 10\ \mu\text{m}$. Thicker samples require freezing at high pressure (about 2,000 bar) that lowers the freezing rate of water and suppresses the formation of cubic ice up to a freezing depth of $\approx 100\ \mu\text{m}$ (66). Cryo-sectioning turned out to be a demanding technique that found its way into other laboratories only slowly. But ultrathin sections of native frozen-hydrated cells, and imaging based on the contrast of untreated biological material only, almost instantly succeeded to clarify open questions of the cell wall architecture in bacteria. Valério Matias and Terry Beveridge demonstrated a periplasmic space in the gram-positives *Bacillus subtilis* and *Staphylococcus aureus* (67, 68), and two other groups showed the bilayer structure of the peculiar outer membrane in mycobacteria and corynebacteria (69, 70), which was not obvious in conventional preparations (71, 72).

Cryo-sectioning is not free of artifacts. Forces acting during the cutting process have various consequences for the frozen sections (73, 74). The most severe disadvantage is compression in the cutting direction that affects the morphology of the cell envelope and the bilayer structure of membranes (Fig. 4, (69)). Although it is

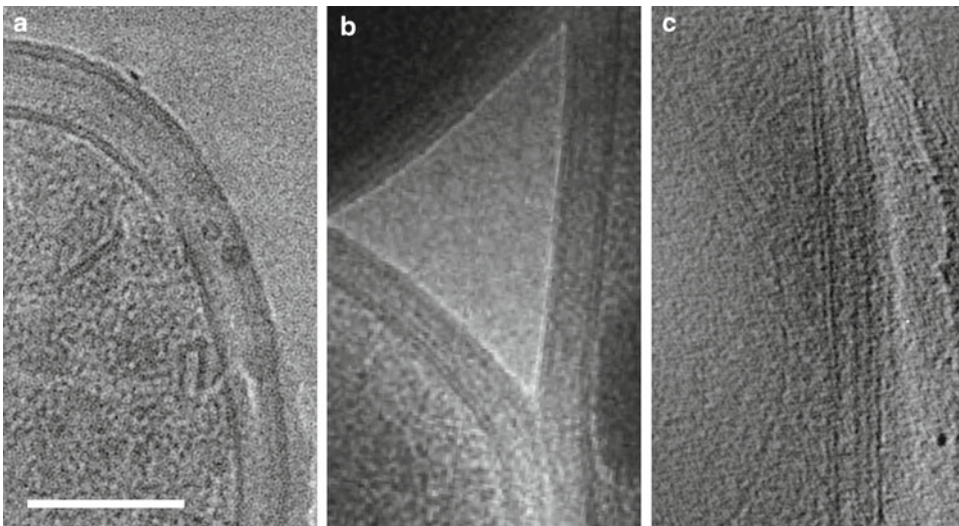


Fig. 4. Mycobacterial cell envelope in cryo-electron microscopy. (a) Cryo-section (thickness $\approx 35\ \text{nm}$), the membrane bilayer structure is preserved perpendicular to and compressed in the cutting direction (from the right). (b) EM projection of a cell thinned by cryo-FIB milling; the bilayer is visible in all orientations but displayed with lower contrast due to the specimen thickness ($\approx 300\ \text{nm}$). (c) Cryo-electron tomography of an intact cell, x - y -slice from the tomogram. Bar indicates 100 nm.

possible to detect periplasmic protein complexes in less squeezed regions of the cell (75) a thinning method without compression effects was desirable for studies of microbial cell envelopes.

3.3. Cryo-Focused Ion Beam Micromachining (Cryo-FIB): Thinning Without Artifacts

Dual beam scanning electron microscopes are equipped with an electron gun and an ion gun (gallium) in addition that is used to abrade material from specimens in a controlled manner. This milling technique is wellknown from material science and was applied to plastic-embedded cells and tissues for imaging by SEM (76, 77). Michael Marko and colleagues described the first experiments with frozen-hydrated bacteria thinned by FIB milling for further investigation in the EM (78, 79). Cryo-FIB has meanwhile been optimized for 2D and 3D electron microscopy and was shown to completely avoid compression of frozen samples and membrane structures (Fig. 4, (80, 81)). Specimen thinning by FIB micromachining will likely become a key technique for the investigation of prokaryotic (and eukaryotic) cells and for cryo-electron tomography in particular (see Subheading 5).

Methods for imaging surfaces and EM of ultrathin sections essentially provide structural information in two dimensions only, either in x - y - (surfaces) or in x - z -direction (thin sections). The development of 3D techniques, covering all dimensions (x , y , z), thus denoted a major step in EM.

4. Macromolecules and Protein Assemblies in Three Dimensions

4.1. Negative Staining of Isolated Protein Complexes

Metal-coating by thermo-electric evaporation provided sufficient contrast for EM but was not suited to yield structural information from all orientations of isolated macromolecules and protein assemblies. The idea to embed particles in heavy metal salts such as Na/K-phosphotungstate (82) and others introduced later (see ref. 83 for a compilation) opened the new field of molecular EM. The technique of negative staining avoided drastic flattening on the specimen support upon drying and stabilized the protein complexes in the electron beam (83, 84). Negatively stained virus capsids (85) and large enzymes (86, 87) were the first molecular specimens that could be reconstructed in 3D. While the investigation of a single negatively stained protein molecule was insufficient, reconstructions including averaging procedures provoked the development of 3D electron microscopy (88) and image processing systems (89–93). Averaging exploits the structural redundancy of regular assemblies such as filamentous and 2D crystalline structures, or uses high numbers of individual molecules, imaged from different projection directions, in single particle approaches.

Negative staining not only opened the door to the third dimension in EM but also improved the resolution of molecular details. The apparent resolution limit of 1.3 nm (83) corresponds to the

diameter of a globular protein domain consisting of eight amino acids (94). This was good enough to get insight into the architecture of filamentous and 2D crystalline protein assemblies. 3D reconstructions of S-layers showed common architectural principles and the variability of the outer surface (95–98) and inspired the search for individual and general functions (29, 99, 100). Studies on major outer membrane proteins in isolated cell walls and reconstituted in artificial 2D crystals clarified the arrangement of pores in trimeric porins (101, 102) before cryo-electron microscopy pushed the resolution limit further (103, 104) and X-ray crystallography succeeded to solve the atomic structure (105). Major contributions to the basic understanding of bacterial appendages concerned the helical organization of flagellins in the flagellar filament and hook (106, 107) and of spirillin in a large basal disk of the *Wolinella succinogenes* flagellar apparatus forming an Archimedian spiral (108).

Although the 3D reconstruction of negatively stained protein complexes and membranous structures was a major step in EM, and the future of the contrast-enhancing technique was regarded optimistic in the early 1990 (83), its application has several drawbacks. (1) Negative staining only offers access to the *shape* of molecules to about 1.3–1.7 nm resolution, but not to its intrinsic structure. (2) Complexes embedded in membranes cannot be stained, only their domains outside of the lipid bilayer and large pores. (3) Artificial variability of protein complexes introduced by embedding in stain, i.e., in high salt concentrations upon drying, and accompanying effects of positive staining can hardly be identified, which affects the interpretation of structural features (109). To overcome the limitations, negative staining was occasionally replaced by polyhydrated compounds (e.g., glucose, erythrose, glycerol) often conjugated with gold (aurothioglucose (110)) or other metal clusters (111). The resolution and structural preservation was considerably increased, but now the specimens became radiation sensitive and enforced low dose microscopy resulting in images of low signal-to-noise ratio. Glucose embedding was extremely successful with the 2D crystalline bacteriorhodopsin still residing in the natural lipid membrane (112). Soluble proteins required a more general approach that consequently led to cryo-electron microscopy of proteins embedded in vitreous ice without contrast-enhancing additives. Negative staining, thus, lost its importance for molecular 3D EM (Fig. 2.1) but is still esteemed for its simplicity and fast application in preparation control and for preliminary structural investigations.

4.2. Cryo-Electron Microscopy: High-Resolution Structures of Regular Assemblies and Single Particles

Frozen-hydrated samples smoothly replaced negatively stained preparations in single particle EM when the microscopes became accessible to remote control and image processing faster due to powerful computers. Although cryo-EM is much more costly and laborious, it has unbeatable advantages. (1) The image signal originates from the biological material, (2) the macromolecules

are embedded in their natural environment (water) and do not experience treatments other than vitrification, (3) the resolution is not limited by any staining and can potentially reach the quasi-atomic level (113).

The low signal-to-noise ratio of images of radiation-sensitive macromolecules requires averaging of 10^3 – 10^6 particles, depending on the number of identical subunits per particle, the intrinsic conformational variability of protein complexes that enforces classification into structural subsets (114, 115), and the resolution desired. If proteins are organized in a regular pattern, alignment and averaging is particularly effective. This was demonstrated and exploited with the first quasi-atomic structure of a 2D crystalline membrane protein, i.e., bacteriorhodopsin (116). The next high-resolution structures were the result of the consequent application of cryo-EM with filamentous structures, where the protein units occur in a helical arrangement. The benefit of such protein filaments is that one EM image already contains projections of the repeating unit in different orientations that can be combined to a 3D electron density map (117–119). The structures of the flagellar filament (120–124) and the hook (125–127) were solved to near-atomic resolution. Some of the latter models were obtained from cryo-EM 3D-reconstructions combined with the X-ray structure of isolated (truncated) flagellin by means of molecular docking. This synergetic combination of techniques, the *hybrid approach* (128–130), has meanwhile become a common strategy to solve the atomic structure of large, flexible and very complex protein assemblies that cannot be crystallized as a whole. A number of other helical appendages (fimbriae, pili) were also investigated by cryo-EM in a similar way (131). Isolated flagellar motors and the switch complex (132–134), periplasmic and outer membrane components of, e.g., the type III (135, 136) and type IV secretion machineries (137, 138), and other periplasmic multicomponent complexes are not filamentous or helical but possess an internal rotational symmetry so that the 3D reconstruction is facilitated in the course of averaging individual particles, again leading to high-resolution models in combination with other methods of protein structure research.

The single particle approach in cryo-EM is a powerful method that will—together with X-ray crystallography—contribute to solve the structure of protein complexes and molecular machines isolated from microbial cell surfaces in the years to come.

5. Cells in Three Dimensions

5.1. Cryo-Electron Tomography (CET): The Integrative Approach

The 3D reconstruction of an individual biological structure is obtained by the tomographic approach. The specimen is tilted around an axis from ideally -90° to $+90^\circ$ (less in practice) and projected every 1° – 3° to collect a 3D data set (tilt series). The projections are aligned

and the 3D electron density map (tomogram) calculated. The basic principles are known since the late 1960s (86, 139). But only when the technical progress allowed for automatic control of electron microscopes (140, 141), electron energy filtering (142, 143), recording of data by sensitive cameras, and demanding computations, it became possible to realize the vision of reconstructing an entire cell in three dimensions. The group of Wolfgang Baumeister pioneered the development of cryo-electron tomography for frozen-hydrated cells in a close-to-life state and is continuing to improve it (65, 144–147). The major characteristics of cryo-tomograms are: (1) they contain the signatures of the entire proteome of a cell, (2) they present the positions, orientations, and interactions of macromolecular complexes in a “snapshot” of a close-to-life situation, (3) they allow to trace intracellular filaments (the cytoskeleton) and large macromolecular assemblies in 3D and to visualize the spatial organization of the cytoplasm and the cell envelope at macromolecular dimensions. Challenges are (1) the low signal-to-noise ratio of original data, (2) the resolution-limiting imaging conditions (defocus), (3) the crowded nature of intact cells with very high concentrations of macromolecules and a heterogeneous composition, making the identification of individual molecules demanding, and (4) the uniqueness of cells that prevents signal enhancement by averaging (except for redundant molecules contained in tomograms, see Subheading 5.3). A comprehensive compilation of the technical aspects of CET is found in (65). The presentation of structural details in the cellular context and in a close-to-life state provides unprecedented insight into the complete 3D organization of cells and new findings in almost all of the reconstructions of bacteria published to date. These include microbial S-layers (148), the mycobacterial outer membrane (69), extracellular membrane vesicles (149), the peptidoglycan (150), the bacterial flagellar apparatus (151–153), the membrane-bound cytoskeleton mediating cell motion in mollicutes (154), and a rapidly growing number of cytoplasmic structures; for selected reviews and articles see refs. 155–159.

It is the fate of new methods that they have to reproduce already established knowledge and to prove that they are able to confirm previous discoveries. Usually, membranes are only reconstructed as solid structures in CET (150, 152, 157), not revealing the lipid bilayer characteristics that are well known from ultrathin sectioning since decades. This is due to extreme underfocus conditions, producing high contrast, but limiting the resolution to about 4–6 nm. However, it is possible to adjust the imaging conditions appropriately and to reconstruct the lipid bilayer of inner and outer membranes (69). In addition, attempts have been made to correct for the focus effects (i.e., for oscillations of the contrast transfer function) by image processing and to enhance the resolution of 3D reconstructions to 2 nm or better (160, 161). Theoretically, it is possible to amend the contrast transfer function already in the

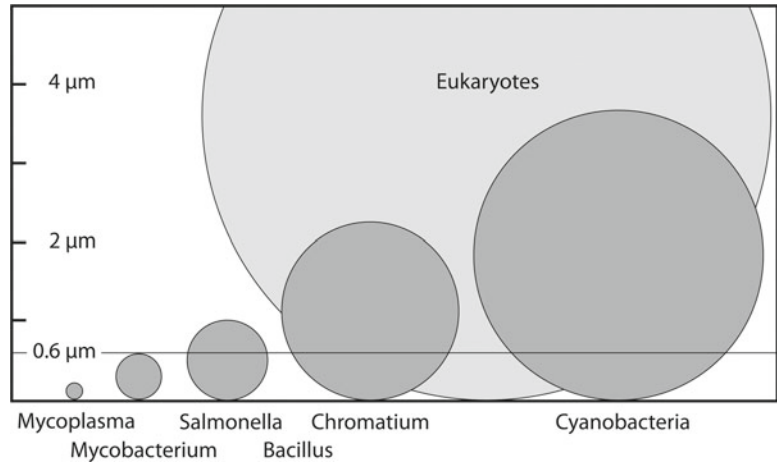


Fig. 5. Scheme of bacterial cell sizes and suitable specimen thickness for cryo-electron tomography (0.6 μm).

microscope in the course of imaging. Recent studies evaluated experimental approaches that appear to be promising and will directly extend the usable resolution for CET (162, 163).

One important limitation is the suitable specimen thickness for tomographic reconstructions. Since electrons strongly interact with atoms the thickness of biological material should ideally not exceed $\approx 0.6 \mu\text{m}$ (0.5–1.0 μm) with 300 keV electron microscopes, the instruments commonly used for cellular CET (65). This limits direct CET applications to an adequate group of microbes and requires thicker cells to be thinned (Fig. 5). As outlined in Subheading 3.3, the method of choice will be FIB milling since it does not only allow to abrase material without compression artifacts but also to cut out lamella from cells in arbitrary positions and orientations (81).

5.2. Correlative Cryo-Microscopy

The inspection and definition of cellular structures in tomograms is feasible by eye or automated segmentation (146, 164) if they are large and characteristic enough (e.g., membranes, filamentous aggregates, flagellar motor). However, the unambiguous identification of (smaller) molecular complexes requires specific labeling or comparison with known structures by an objective approach. Classical labeling with immunogold is possible for surface structures of intact cells that are accessible from outside. The widely applied label green fluorescent protein (GFP) is not directly detectable by electron microscopy. But it can be used to identify subregions of big cells or individual bacteria in multicellular aggregates (consortia) by cryo-fluorescence microscopy for selective thinning by FIB and/or imaging by CET. The *correlative microscopy* approach (80, 81, 165) has been developed in recent years and is advantageous for selecting appropriate cells or cellular regions in

an efficient manner for CET. Recently, fusion of proteins with electron-dense ferritin was achieved and can directly be applied to find labeled proteins in tomograms (166).

However, any labeling may modify native interactions with other macromolecules; it would thus be desirable if unaltered protein complexes were detectable by their individual structures. This is accomplished by *template matching*.

5.3. Combining CET and Single Particle Averaging: The Template Matching Approach

Tomograms contain the signatures of the entire proteome being present in the reconstructed volume. Provided that the signal of a protein complex of interest is strong enough it can be detected and identified by cross-correlating tomograms with the 3D structure of the molecule (167–169). The template may originate from X-ray crystallography or single particle EM (see Subheading 4.2). Examples for soluble protein complexes in bacteria demonstrate the potential of the approach (159, 170). It needs some effort to extract the high-resolution information of tomograms and to selected sub-tomograms containing the identified protein complexes. But the combination of artifact-free cryo-preparations of cells and cell membranes in particular, appropriate imaging conditions and of image processing approaches, correcting for contrast variations due to focus conditions and the focus gradient in projections of the tilted specimen (160), promises to get insight into the structure of membrane (and other) protein complexes to 1–1.5 nm resolution (171). Template matching finds the positions and orientations of the respective protein complexes that can be extracted (sub-tomograms) and 3D averaged afterwards. If the sub-volumes include some neighboring space specifically interacting structures will be captured in an in situ situation. By this way labile or only temporarily existing but functional protein aggregations may be identified and structurally investigated.

6. Perspectives

Future investigations of bacterial structures will reside in the cold and will predominantly make use of 3D information. Cryo-electron tomography and its associated techniques will take over what electron microscopy of ultrathin sections of plastic-embedded material has been for structural research in microbiology for the last four decades. The goal is to visualize whole cells at molecular resolution and to evaluate molecular interactions in situ. The template matching approach is still in its beginning and awaits broader application in the years to come. The challenge is the reliable identification of smaller protein complexes in the crowded cytoplasm and in membranes, which would benefit from electron detectors with improved signal transformation in the higher resolution range and from more efficient correction approaches for the contrast transfer function in

the course of 3D reconstruction. The introduction of commercial solutions for cryo-FIB micromachining and phase-corrected electron microscopy employing phase plates could denote a further step forward. With these improvements, the perspectives to successfully explore the largely uncharted territories of the bacterial cell envelope—the periplasm and the outer (and inner) membrane *in situ*—are promising.

References

1. van Leeuwenhoek A (1684) Microscopical observations about animals in the scurf of the teeth, the substance called jvorms in the nose, and the cuticula consisting of scales. *Phil Transact Royal Soc* 159:308
2. Ehrlich P (1882) *Deut Med Wochenschr* 8:269–270
3. Gram HC (1884) Über die isolierte Färbung der Schizomyceten in Schnitt- und Trockenpräparaten. *Fortschr Med* 2:185–189
4. Salton MRJ (1964) The bacterial cell wall. American Elsevier Publ Co, New York
5. Beveridge TJ (1990) Mechanism of gram variability in selected bacteria. *J Bacteriol* 172:1609–1620
6. Popescu A, Doyle RJ (1996) The gram stain after more than a century. *Biotech Histochem* 71:145–151
7. White PB (1926) Further studies of the *Salmonella* group. Great Britain Medical Research Council 103, p 3–160
8. Salmonella Subcommittee (1934) *J Hyg* 34:333–350
9. Grimont PAD, Weill FX (2007) Antigenic formulae of the *Salmonella* serovars, 9th edn. World Health Organization Collaborating Centre for Reference and Research on Salmonella, Institut Pasteur, Paris
10. Knoll M, Ruska E (1932) Das Elektronenmikroskop. *Z Phys* 78:318–339
11. Krause F (1937) Das magnetische Elektronenmikroskop und seine Anwendung in der Biologie. *Naturwissenschaften* 25:817–825
12. Marton L (1937) La microscopie électronique des objets biologiques. *Bull Acad Roy Belg Cl Sci* 23:672–678
13. Knaysi G (1949) Cytology of bacteria II. *Bot Rev* 15:106–151
14. Chapman GB, Hillier J (1953) Electron microscopy of ultra-thin sections of bacteria I. Cellular division in *Bacillus cereus*. *J Bacteriol* 66:362–373
15. Houwink AL (1953) A macromolecular monolayer in the cell wall of *Spirillum* spec. *Biochim Biophys Acta* 10:360–366
16. Müller HO (1942) Die Ausmessung der Tiefe übermikroskopischer Objekte. *Kolloid-Zeitschrift* 99:6–28
17. Williams RC, Wyckoff RWG (1945) Electron shadow micrography of the tobacco mosaic virus protein. *Science* 101:594–596
18. Houwink AL (1956) Flagella, gas vacuoles and cell-wall structure in *Halobacterium halobium*; an electron microscope study. *J Gen Microbiol* 15:146–150
19. Wildhaber I, Gross H, Engel A, Baumeister W (1985) The effects of air-drying and freeze-drying on the structure of a regular protein layer. *Ultramicroscopy* 16:411–422
20. Guckenberger R (1985) Surface reliefs derived from heavy-metal-shadowed specimens—Fourier space technique applied to periodic objects. *Ultramicroscopy* 16:357–370
21. Engelhardt H, Guckenberger R, Hegerl R, Baumeister W (1985) High resolution shadowing of freeze-dried bacterial photosynthetic membranes: multivariate statistical analysis and surface relief reconstruction. *Ultramicroscopy* 16:395–410
22. Baumeister W, Guckenberger R, Engelhardt H, Woodcock CLF (1986) Metal shadowing and decoration in electron microscopy of biological macromolecules. *Ann N Y Acad Sci* 483:57–76
23. Wildhaber I, Hegerl R, Barth M, Gross H, Baumeister W (1986) Three-dimensional reconstruction of a freeze-dried and metal-shadowed bacterial surface layer. *Ultramicroscopy* 19:57–68
24. Bachmann L, Becker R, Leupold G, Barth M, Guckenberger R, Baumeister W (1985) Decoration and shadowing of freeze-etched catalase crystals. *Ultramicroscopy* 16:305–320
25. Rübenkamm E, Braun N, Bachmann L, Bacher A, Brandt J, Baumeister W, Weinkauff S (1995) Quantitative evaluation of heavy metal decoration on protein molecules: contrast, specificity and resolution. *Ultramicroscopy* 58:337–351
26. Moor H, Mühlethaler K, Waldner H, Frey-Wyssling A (1961) A new freezing-ultramicrotome. *J Biophys Biochem Cytol* 10:1–13

27. Reimer L, Schulte C (1966) Elektronenmikroskopische Oberflächenabdrücke und ihr Auflösungsvermögen. *Naturwissenschaften* 53:489–497
28. Holt SC, Trüper HG, Takács BJ (1968) Fine structure of *Ectothiorhodospira mobilis* strain 8113 thylakoids: chemical fixation and freeze-etching studies. *Arch Mikrobiol* 62:111–128
29. Engelhardt H (2007) Are S-layers exoskeletons? The basic function of surface protein layers revisited. *J Struct Biol* 160:115–124
30. Sleytr U, Adam H, Klaushofer H (1969) Die Feinstruktur der Zellwand und Cytoplasmamembran von *Clostridium nigrificans*, dargestellt mit Hilfe der Gefrierätz- und Ultradünnschnitttechnik. *Arch Mikrobiol* 66:40–58
31. Holt SC, Beveridge TJ (1982) Electron microscopy: its development and application to microbiology. *Can J Microbiol* 28:1–53
32. Schatten H (2011) Low voltage high-resolution SEM (LVHRSEM) for biological structural and molecular analysis. *Micron* 42:175–185
33. Binnig G, Rohrer H, Gerber C, Weibel E (1982) Surface studies by scanning tunneling microscopy. *Phys Rev Lett* 49:57–61
34. Binnig G, Quate CF, Gerber C (1986) Atomic force microscope. *Phys Rev Lett* 56:930–933
35. Wiegräbe W, Nonnenmacher M, Guckenberger R, Wolter O (1991) Atomic force microscopy of a hydrated bacterial surface protein. *J Microsc* 163:79–84
36. Müller DJ, Baumeister W, Engel A (1996) Conformational change of the hexagonally packed intermediate layer of *Deinococcus radiodurans* monitored by atomic force microscopy. *J Bacteriol* 178:3025–3030
37. Schabert FA, Henn C, Engel A (1995) Native *Escherichia coli* OmpF porin surfaces probed by atomic force microscopy. *Science* 268:92–94
38. Engel A, Schoenenberger C-A, Müller DJ (1997) High resolution imaging of native biological sample surfaces using scanning probe microscopy. *Curr Opin Struct Biol* 7:279–284
39. Scheuring S, Müller DJ, Stahlberg H, Engel H-A, Engel A (2002) Sampling the conformational space of membrane protein surfaces with the AFM. *Eur Biophys J* 31:172–178
40. Philippssen A, Im W, Engel A, Schirmer T, Roux B, Müller DJ (2002) Imaging the electrostatic potential of transmembrane channels: atomic probe microscopy of OmpF porin. *Biophys J* 82:1667–1676
41. Knapp HF, Wiegräbe W, Heim M, Eschrich R, Guckenberger R (1995) Atomic force microscope measurements and manipulation of Langmuir-Blodgett films with modified tips. *Biophys J* 69:708–715
42. Gonçalves RP, Scheuring S (2006) Manipulating and imaging individual membrane proteins by AFM. *Surf Interface Anal* 38:1413–1418
43. Müller DJ (2008) AFM: a nanotool in membrane biology. *Biochemistry* 47:7986–7998
44. Anselmetti D, Hansmeier N, Kalinowski J, Martini J, Merkle T, Pamisano R, Ros R, Schmied K, Sischka A, Toensing K (2007) Analysis of subcellular surface structures, function and dynamics. *Anal Bioanal Chem* 387:83–89
45. Marton L (1976) Early application of electron microscopy to biology. *Ultramicroscopy* 1:281–296
46. Baker RF, Pease DC (1949) Sectioning of the bacterial cell for the electron microscope. *Nature* 163:282
47. Sjöstrand FS (1953) A new microtome for ultrathin sectioning for high resolution electron microscopy. *Experientia* 9:114–115
48. Kellenberger E, Ryter A (1958) Cell wall and cytoplasmic membrane of *Escherichia coli*. *J Biophys Biochem Cytol* 4:323–326
49. Murray RGE (1963) On the cell wall structure of *Spirillum serpens*. *Can J Microbiol* 9:381–392
50. Claus GW, Roth LE (1964) Fine structure of the gram-negative bacterium *Acetobacter suboxydans*. *J Cell Biol* 20:217–233
51. Costerton JW (1979) The role of electron microscopy in the elucidation of bacterial structure and function. *Annu Rev Microbiol* 33:459–479
52. Sleytr UB (1978) Regular arrays of macromolecules on bacterial cell walls: structure, chemistry, assembly, and function. *Int Rev Cytol* 53:1–64
53. Remsen CC, Watson SW, Trüper HG (1970) Macromolecular subunits in the walls of marine photosynthetic bacteria. *J Bacteriol* 103:254–257
54. Hageage GJ, Gherna RL (1971) Surface structure of *Chromatium okenii* and *Chromatium weissei*. *J Bacteriol* 106:687–690
55. Jeffries P, Wilkinson JF (1978) Electron microscopy of the cell wall complex of *Methylobionas albus*. *Arch Microbiol* 119:227–229
56. Murray RGE (1978) Form and function. In: Norris JR, Richmond MH (eds) *Essays in microbiology. I Bacteria*. Wiley, New York, pp 2/30–2/31
57. Emde B, Wehrli E, Baumeister W (1980) The topography of the cell wall of *Micrococcus*

- radiodurans*. In: Brederoo P, de Priester W (ed) Proc 7th Europ Congr Electron Microscopy, vol. 2, Leiden, 1980, p 460–461
58. Graham LL, Beveridge TJ (1990) Evaluation of freeze-substitution and conventional embedding protocols for routine electron microscopic processing of eubacteria. *J Bacteriol* 172:2141–2149
 59. Tokunaga M, Kusamichi M, Koike H (1986) Ultrastructure of outermost layer of cell wall in *Candida albicans* observed by rapid-freezing technique. *J Electron Microsc* 35:237–246
 60. Fernández-Morán H (1960) Low-temperature preparation techniques for electron microscopy of biological specimens based on rapid freezing with liquid Helium II. *Ann N Y Acad Sci* 85:689–713
 61. Dubochet J, McDowell AW, Menge B, Schmid EN, Lickfeld KG (1983) Electron microscopy of frozen-hydrated bacteria. *J Bacteriol* 155:381–390
 62. Al-Amoudi A, Chang J-J, Leforestier A, McDowell A, Salamin LM, Norlén LPO, Richter K, Blanc NS, Studer D, Dubochet J (2004) Cryo-electron microscopy of vitreous sections. *EMBO J* 23:3583–3588
 63. Dubochet J (2012) Cryo-EM—the first thirty years. *J Microsc* 245:221–224
 64. Dubochet J, McDowell AW (1981) Vitrification of pure water for electron microscopy. *J Microsc* 124:RP3–RP4
 65. Plitzko JM, Baumeister W (2007) Cryoelectron tomography (CET). In: Hawkes PW, Spence JCH (eds) *Science of microscopy*, vol I. Springer, New York, pp 535–604
 66. Shimon E, Müller M (1998) On optimizing high-pressure freezing: from heat transfer theory to a new microbiopsy device. *J Microsc* 192:236–247
 67. Matias VRF, Beveridge TJ (2005) Cryo-electron microscopy reveals native polymeric cell wall structure in *Bacillus subtilis* 168 and the existence of a periplasmic space. *Mol Microbiol* 56:240–251
 68. Matias VRF, Beveridge TJ (2006) Native cell wall organization shown by cryo-electron microscopy confirms the existence of a periplasmic space in *Staphylococcus aureus*. *J Bacteriol* 188:1011–1021
 69. Hoffmann C, Leis A, Niederweis M, Plitzko JM, Engelhardt H (2008) Disclosure of the mycobacterial outer membrane: cryo-electron tomography and vitreous sections reveal the lipid bilayer structure. *Proc Natl Acad Sci U S A* 105:3963–3967
 70. Zuber B, Chami M, Houssin C, Dubochet J, Griffith G, Daffé M (2008) Direct visualization of the outer membrane of mycobacteria and corynebacteria in their native state. *J Bacteriol* 190:5672–5680
 71. Paul TR, Beveridge TJ (1992) Reevaluation of envelope profiles and cytoplasmic ultrastructure of mycobacteria processed by conventional embedding and freeze-substitution protocols. *J Bacteriol* 174:6508–6517
 72. Bleck CKE, Merz A, Gutierrez MG, Walther P, Dubochet J, Zuber B, Griffith G (2009) Comparison of different methods for thin sections EM analysis of *Mycobacterium smegmatis*. *J Microsc* 237:23–38
 73. Al-Amoudi A, Studer D, Dubochet J (2005) Cutting artefacts and cutting process in vitreous sections for cryo-electron microscopy. *J Struct Biol* 150:109–121
 74. Han H-M, Zuber B, Dubochet J (2008) Compression and crevasses in vitreous sections under different cutting conditions. *J Microsc* 230:167–171
 75. Zuber B, Haenni M, Ribeiro T, Minnig K, Lopes F, Moreillon P, Dubochet J (2006) Granular layer in the periplasmic space of gram-positive bacteria and fine structures of *Enterococcus gallinarum* and *Streptococcus gordonii* septa revealed by cryo-electron microscopy of vitreous sections. *J Bacteriol* 188:6652–6660
 76. Ballerini M, Milani M, Batani M, Squadrini F (2001) Focused ion beam techniques for the analysis of biological samples: a revolution in ultramicroscopy? *Proc SPIE* 4261:92–104
 77. Heymann JAW, Hayles M, Gestmann I, Giannuzzi LA, Lich B, Subramaniam S (2006) Site-specific 3D imaging of cells and tissues with a dual beam microscope. *J Struct Biol* 155:63–73
 78. Marko M, Hsieh C, Moberlychan W, Mannella CA, Frank J (2006) Focused ion beam milling of vitreous water: prospects for an alternative to cryo-ultramicrotomy of frozen-hydrated biological samples. *J Microsc* 222:42–47
 79. Marko M, Hsieh C, Schalek R, Frank J, Mannella C (2007) Focused-ion-beam thinning of frozen-hydrated biological specimens for cryo-electron microscopy. *Nat Methods* 4:2015–2017
 80. Rigort A, Bäuerlein FJB, Leis A, Gruska M, Hoffmann C, Laugks T, Böhm U, Eibauer M, Gnaegi H, Baumeister W, Plitzko JM (2010) Micromachining tools and correlative approaches for cellular cryo-electron tomography. *J Struct Biol* 172:169–179
 81. Rigort A, Bäuerlein FJB, Villa E, Eibauer M, Laugks T, Baumeister W, Plitzko JM (2012) Focused ion beam micromachining of

- eukaryotic cells for cryoelectron tomography. *Proc Natl Acad Sci U S A* 109:4449–4454
82. Brenner S, Horne RW (1959) A negative staining method for high resolution electron microscopy of viruses. *Biochim Biophys Acta* 34:103–110
 83. Bremer A, Henn C, Engel A, Baumeister W, Aepli U (1992) Has negative staining still a place in biomacromolecular electron microscopy? *Ultramicroscopy* 46:85–111
 84. Anderson TF (1962) Negative staining and its use in the study of viruses and their serological reactions. In: Harris RJC (ed) *Symposium of the international society for cell biology*, vol 1. Academic, New York, pp 251–262
 85. DeRosier DJ, Klug A (1968) Reconstruction of three-dimensional structures from electron micrographs. *Nature* 217:130–134
 86. Hoppe W, Langer R, Knesch G, Poppe C (1968) Proteinkristallstrukturanalyse mit Elektronenstrahlen. *Naturwissenschaften* 55:333–336
 87. Hoppe W, Gassmann J, Hunsmann N, Schramm HJ, Sturm M (1974) Three-dimensional reconstruction of individual negatively stained yeast fatty-acid synthetase molecules from tilt series in the electron microscope. *Hoppe Seylers Z Physiol Chem* 355:1483–1487
 88. Frank J (1989) Image analysis of single molecules. *Electron Microsc Rev* 2:53–74
 89. Hegerl R (1996) The EM program package: a platform for image processing in biological electron microscopy. *J Struct Biol* 116:30–34
 90. van Heel M, Harauz G, Orlova EV, Schmidt R, Schatz M (1996) A new generation of the IMAGIC image processing system. *J Struct Biol* 116:17–24
 91. Sorzano COS, Marabini R, Velázquez-Muriel J, Bilbao-Acstro JR, Scheres SHW, Carazo JM, Pascual-Montano A (2004) XMIPP: a new generation of an open-source image processing package for electron microscopy. *J Struct Biol* 148:194–204
 92. Shaik TR, Gao H, Baxter WT, Asturias FJ, Boisset N, Leith A, Frank J (2008) SPIDER image processing for single-particle reconstruction of biological macromolecules from electron micrographs. *Nat Protoc* 3:1941–1974
 93. Korinek A, Beck F, Baumeister W, Nickell S, Plitzko JM (2011) Computer controlled cryo-electron microscopy—TOM² a software package for high-throughput applications. *J Struct Biol* 175:394–405
 94. Engelhardt H (1991) Electron microscopy of microbial cell wall proteins. Surface topography, three-dimensional reconstruction, and strategies for two-dimensional crystallization. In: Latgé JP, Boucias D (eds) *Fungal cell wall and immune response*, NATO ASI Series H53. Springer, Berlin, pp 11–25
 95. Saxton WO, Baumeister W, Hahn M (1984) Three-dimensional reconstruction of imperfect two-dimensional crystals. *Ultramicroscopy* 13:57–70
 96. Bingle WH, Engelhardt H, Page WJ, Baumeister W (1987) Three-dimensional structure of the regular tetragonal surface layer of *Azotobacter vinelandii*. *J Bacteriol* 169:5008–5015
 97. Engelhardt H, Cejka Z, Baumeister W (1988) Three-dimensional structure of surface layers from various *Bacillus* and *Clostridium* species. In: Sleytr UB, Messner P, Pum D, Sára M (eds) *Crystalline bacterial cell surface layers*. Springer, Berlin, pp 87–91
 98. Tsuboi A, Engelhardt H, Santarius U, Tsukagoshi N, Uda S, Baumeister W (1989) Three-dimensional structure of the surface protein layer (MW layer) of *Bacillus brevis* 47. *J Ultrastruct Mol Struct Res* 102:178–187
 99. Beveridge TJ, Pouwels PH, Sára M et al (1997) Functions of S-layers. *FEMS Microbiol Rev* 20:99–149
 100. Engelhardt H, Peters J (1998) Structural research on surface layers—a focus on stability, surface layer homology domains, and surface layer-cell wall interactions. *J Struct Biol* 124:276–302
 101. Engel A, Massalski A, Schindler H, Dorset DL, Rosenbusch JP (1985) Porin channel triplets merge into single outlets in *Escherichia coli* outer membranes. *Nature* 317:643–645
 102. Chalcroft JP, Engelhardt H, Baumeister W (1987) Structure of the porin from a bacterial stalk. *FEBS Lett* 211:53–58
 103. Sass JJ, Massalski A, Beckmann E, Büldt G, Dorset D, van Heel M, Rosenbusch JP, Zeitler E, Zemlin F (1988) High-resolution cryomicroscopy of porin (OmpF). In: Bailey GW (ed) *Proc 46th Ann Meet Electron Microscopy Soc Am*. San Francisco Press, San Francisco, pp 146–147
 104. Jap B, Downing KH, Walian PJ (1990) Structure of PhoE porin in projection at 3.5 Å resolution. *J Struct Biol* 103:57–63
 105. Weiss MS, Abele U, Weckesser J, Welte W, Schiltz E, Schulz GE (1991) Molecular architecture and electrostatic properties of a bacterial porin. *Science* 254:1627–1630
 106. Trachtenberg S, DeRosier DJ, Macnab RM (1987) Three-dimensional structure of the complex flagellar filament of *Rhizobium lupini*

- and its relation to the structure of the plain filament. *J Mol Biol* 195:603–620
107. Morgan DG, Machnab RM, Francis NR, DeRosier DJ (1993) Domain organization of the subunit of the *Salmonella typhimurium* flagellar hook. *J Mol Biol* 229:79–84
 108. Engelhardt H, Schuster SC, Baeuerlein E (1993) An Archimedian spiral: the basal disk of the *Wolinella* flagellar hook. *Science* 262:1046–1048
 109. Woodcock CL, Baumeister W (1990) Different representations of a protein structure obtained with different negative stains. *Eur J Cell Biol* 51:45–52
 110. Rachel R, Jakubowski U, Tietz H, Hegerl R, Baumeister W (1986) Projected structure of the surface protein of *Deinococcus radiodurans* determined to 8 Å resolution by cryomicroscopy. *Ultramicroscopy* 20:305–316
 111. Jakubowski U, Hegerl R, Formanek H, Volker S, Santarius U, Baumeister W (1988) Three-dimensional reconstruction of the HPI-layer of *Deinococcus radiodurans* embedded in Cd-thioglycerol. *Inst Phys Conf Ser* 93(3):381–382
 112. Henderson R, Unwin PNT (1975) Three-dimensional model of purple membrane obtained by electron microscopy. *Nature* 257:28–32
 113. Glaeser RM, Hall RJ (2011) Reaching the information limit in cryo-EM of biological macromolecules: experimental aspects. *Biophys J* 100:2331–2337
 114. Penczek P, Radermacher M, Frank J (1992) Three-dimensional reconstruction of single particles embedded in ice. *Ultramicroscopy* 40:33–52
 115. Frank J, Radermacher M (1992) Three-dimensional reconstruction of single particles negatively stained or in vitreous ice. *Ultramicroscopy* 46:241–262
 116. Henderson R, Baldwin JM, Ceska TA, Zemlin F, Beckmann E, Downing KH (1990) Model for the structure of bacteriorhodopsin based on high-resolution electron cryo-microscopy. *J Mol Biol* 213:899–929
 117. DeRosier DJ, Moore PB (1970) Reconstruction of three-dimensional images from electron micrographs of structures with helical symmetry. *J Mol Biol* 52:355–369
 118. Morgan DG, DeRosier D (1992) Processing images of helical structures: a new twist. *Ultramicroscopy* 46:263–285
 119. Egelman EH (2000) A robust algorithm for the reconstruction of helical filaments using single-particle methods. *Ultramicroscopy* 85:225–234
 120. Mimori Y, Samashita I, Murata K, Fujiyoshi Y, Yonekura K, Toyoshima C, Namba K (1995) The structure of the R-type straight flagellar filament of *Salmonella* at 9 Å resolution by electron cryomicroscopy. *J Mol Biol* 249:69–87
 121. Morgan DG, Owen C, Melanson LA, DeRosier DJ (1995) Structure of bacterial flagellar filaments at 11 Å resolution: packing of the α -helices. *J Mol Biol* 249:88–110
 122. Yonekura K, Maki-Yonekura S, Namba K (2003) Complete atomic model of the bacterial flagellar filament by electron cryomicroscopy. *Nature* 424:643–650
 123. Galkin VE, Yu X, Bielnicki J, Heuser J, Ewing CP, Guerry P, Egelman EH (2008) Divergence of quaternary structures among bacterial flagellar filaments. *Science* 320:382–385
 124. Maki-Yonekura S, Yonekura K, Namba K (2010) Conformational change of flagellin for polymorphic supercoiling of the flagellar filament. *Nat Struct Mol Biol* 17:417–422
 125. Samatey FA, Natsunami H, Imada K, Gagashima S, Shaikh T, Thomas DR, Chen JZ, DeRosier DJ, Kitao A, Namba K (2004) Structure of the bacterial flagellar hook and implication for the molecular universal joint mechanism. *Nature* 431:1062–1068
 126. Shaik TR, Thomas DR, Chen JZ, Samatey FA, Matsunami H, Imada K, Namba K, DeRosier DJ (2005) A partial atomic structure for the flagellar hook of *Salmonella typhimurium*. *Proc Natl Acad Sci U S A* 102:1023–1028
 127. Fujii T, Kato T, Namba K (2009) Specific arrangement of α -helical coiled coils in the core domain of the bacterial flagellar hook for the universal joint function. *Structure* 17:1485–1493
 128. Steven AC, Baumeister W (2008) The future is hybrid. *J Struct Biol* 163:186–195
 129. Wriggers W (2010) Using *Situs* for the integration of multi-resolution structures. *Biophys Rev* 2:21–27
 130. Trabuco LG, Schreiner E, Gumbart J, Hsin J, Villa E, Schulten K (2011) Applications of the molecular dynamics flexible fitting method. *J Struct Biol* 173:420–427
 131. Fujii T, Cheung M, Blanco A, Kato T, Blocker AJ, Namba K (2012) Structure of a type III secretion needle at 7-Å resolution provides insights into its assembly and signaling mechanisms. *Proc Natl Acad Sci U S A* 109:4461–4466
 132. Young HS, Dang H, Lai Y, DeRosier DJ, Khan S (2003) Variable symmetry in *Salmonella typhimurium* flagellar motors. *Biophys J* 84:571–577

133. Thomas DR, Francis NR, Xu C, DeRosier DJ (2006) The three-dimensional structure of the flagellar rotor from a clockwise-locked mutant of *Salmonella enterica* serovar typhimurium. *J Bacteriol* 188:7039–7048
134. Minamino T, Imada K, Namba K (2008) Molecular motors of the bacterial flagella. *Curr Opin Struct Biol* 18:693–701
135. Schraidt O, Lefebvre MD, Brunner MJ, Schmied WH, Schmidt A, Radics J, Mechtler K, Galán JE, Marlovits TC (2010) Topology and organization of the *Salmonella typhimurium* type III secretion needle complex components. *PLoS Pathog* 6:e1000824
136. Schraidt O, Marlovits TC (2011) Three-dimensional model of *Salmonella*'s needle complex at subnanometer resolution. *Science* 331:1192–1195
137. Fronzes R, Schäfer E, Wang L, Saibil HR, Orlova EV, Waksman G (2009) Structure of a type IV secretion system core complex. *Science* 323:266–268
138. Chandran V, Fronzes R, Duquerroy S, Cronin N, Navaza J, Waksman G (2009) Structure of the outer membrane complex of a type IV secretion system. *Nature* 462:1011–1015
139. Hart RG (1968) Electron microscopy of unstained biological material: the polytropic montage. *Science* 159:1464–1467
140. Dierksen K, Typke D, Hegerl R, Koster AJ, Baumeister W (1992) Towards automatic electron tomography. *Ultramicroscopy* 40:71–87
141. Dierksen K, Typke D, Hegerl R, Baumeister W (1993) Towards automatic electron tomography II. Implementation of autofocus and low-dose procedures. *Ultramicroscopy* 49:109–120
142. Grimm R, Koster J, Ziese U, Typke D, Baumeister W (1996) Zero-loss energy filtering under low-dose conditions using a post-column energy filter. *J Microsc* 183:60–68
143. Grimm R, Typke D, Baumeister W (1998) Improving image quality by zero-loss energy filtering: quantitative assessment by means of image cross-correlation. *J Microsc* 190:339–349
144. Medalia O, Weber I, Frangakis AS, Nicastro D, Gerisch G, Baumeister W (2002) Macromolecular architecture in eukaryotic cells visualized by cryoelectron tomography. *Science* 298:1209–1213
145. Baumeister W (2002) Electron tomography: towards visualizing the molecular organization of the cytoskeleton. *Curr Opin Struct Biol* 12:679–684
146. Lucic V, Förster F, Baumeister W (2005) Structural studies by electron tomography: from cells to molecules. *Annu Rev Biochem* 74:833–865
147. Leis A, Rockel B, Andrees L, Baumeister W (2009) Visualizing cells at the nanoscale. *Trends Biochem Sci* 34:60–70
148. Nickell S, Hegerl R, Baumeister W, Rachel R (2003) *Pyrodictium* cannulae enter the periplasmic space but do not enter the cytoplasm, as revealed by cryo-electron tomography. *J Struct Biol* 141:34–42
149. Schrepf H, Koebsch I, Walter S, Engelhardt H, Meschke H (2011) Extracellular *Streptomyces* vesicles: amphorae for survival and defence. *Microb Biotechnol* 4:286–299
150. Gan L, Chen S, Jensen GJ (2008) Molecular organization of Gram-negative peptidoglycan. *Proc Natl Acad Sci U S A* 105:18953–18957
151. Murphy GE, Leadbetter JR, Jensen GJ (2006) In situ structure of the complete *Treponema primitia* flagellar motor. *Nature* 442:1062–1064
152. Izard J, Hsieh C-E, Limberger R, Mannella CA, Marko M (2008) Native cellular architecture of *Treponema denticola* revealed by cryo-electron tomography. *J Struct Biol* 163:10–17
153. Chen S, Beeby M, Murphy GE, Leadbetter JR, Hendrixon DR, Briegel A, Li Z, Shi J, Tocheva EI, Müller A, Dobro MM, Jensen GJ (2011) Structural diversity of bacterial flagellar motors. *EMBO J* 30:2972–2981
154. Kürner J, Frangakis AS, Baumeister W (2005) Cryo-electron tomography reveals the cytoskeletal structure of *Spiroplasma melliferum*. *Science* 307:436–438
155. Jensen GJ, Briegel A (2007) How electron cryotomography is opening a new window onto prokaryotic ultrastructure. *Curr Opin Struct Biol* 17:260–267
156. Morris DM, Jensen GJ (2008) Toward a bio-mechanical understanding of whole bacterial cells. *Annu Rev Biochem* 77:583–613
157. Ting CS, Hsieh C, Sundararaman S, Mannella C, Marko M (2007) Cryo-electron tomography reveals the comparative three-dimensional architecture of *Prochlorococcus*, a globally important marine cyanobacterium. *J Bacteriol* 289:4485–4493
158. Beck M, Malmström JA, Lange V, Schmidt A, Deutsch EW, Aebersold R (2009) Visual proteomics of the human pathogen *Leptospira interrogans*. *Nat Methods* 6:817–823
159. Ortiz JO, Brandt F, Matias VRF, Sennels L, Rappsilber J, Scheres SHW, Eibauer M, Hartl FU, Baumeister W (2010) Structure of

- hibernating ribosomes studied by cryoelectron tomography in vitro and in situ. *J Cell Biol* 190:613–621
160. Fernández JJ, Li S, Crowther RA (2006) CTF determination and correction in electron cryotomography. *Ultramicroscopy* 106: 587–596
 161. Xiong Q, Morphew MK, Schwartz CL, Hoenger AH, Mastronarde DN (2009) CTF determination and correction for low dose tomographic tilt series. *J Struct Biol* 168: 378–387
 162. Danev R, Nagayama K (2001) Transmission electron microscopy with zernike phase plate. *Ultramicroscopy* 88:243–252
 163. Danev R, Kanamaru S, Marko M, Nagayama K (2010) Zernike phase contrast cryo- electron tomography. *J Struct Biol* 171:174–181
 164. Rigort A, Günther D, Hegerl R, Baum D, Weber B, Prohaska S, Medalia O, Baumeister W, Hege H-C (2012) Automated segmentation of electron tomograms for a quantitative description of actin filament networks. *J Struct Biol* 177:135–144
 165. Sartori A, Gatz R, Beck F, Rigort A, Baumeister W, Plitzko JM (2007) Correlative microscopy: bridging the gap between fluorescence light microscopy and cryo-electron tomography. *J Struct Biol* 160:135–145
 166. Wang Q, Mercogliano CP, Löwe J (2011) A ferritin-based label for cellular electron cryotomography. *Structure* 19:147–154
 167. Frangakis AS, Böhm J, Förster F, Nickell S, Nicastro D, Typke D, Hegerl R, Baumeister W (2002) Identification of macromolecular complexes in cryoelectron tomograms of phantom cells. *Proc Natl Acad Sci U S A* 99:14153–14158
 168. Frangakis AS, Förster F (2004) Computational exploration of structural information from cryo-electron tomograms. *Curr Opin Struct Biol* 14:325–331
 169. Nickell S, Kofler C, Leis AP, Baumeister W (2006) A visual approach to proteomics. *Nat Rev Mol Cell Biol* 7:225–230
 170. Ortiz JO, Förster F, Kürner J, Linaroudis AA, Baumeister W (2006) Mapping 70S ribosomes in intact cells by cryoelectron tomography and pattern recognition. *J Struct Biol* 156:334–341
 171. Eibauer M (2011) Korrektur der transferfunktionen CTF und MTF in der Kryoelektronentomographie. Thesis, Technical University of Munich



<http://www.springer.com/978-1-62703-244-5>

Bacterial Cell Surfaces
Methods and Protocols
Delcour, A.H. (Ed.)
2013, XII, 399 p., Hardcover
ISBN: 978-1-62703-244-5
A product of Humana Press